Electronic Supplementary Material (ESI) for Lab on a Chip.

ELECTRONIC SUPPLEMENTARY INFORMATION

Construction of core-shell microcapsules via focused surface acoustic wave microfluidics

Shaobo Jin[a], *Xueyong Wei**[a], *Juan Ren*[a], *Zhuangde Jiang*[a], *Chris Abell*[b] *and Ziyi Yu**[b,c]

[a] State Key Laboratory for Manufacturing Systems Engineering, Xi'an Jiaotong University, Xi'an, 710049, China. E-mail: seanwei@mail.xjtu.edu.cn

[b] Department of Chemistry, University of Cambridge, Lensfield Road, Cambridge CB2 1EW, UK.

[c] State Key Laboratory of Materials-Oriented Chemical Engineering, College of Chemical Engineering, Nanjing Tech University, 30 Puzhu South Road, Nanjing 211816, China.E-mail: ziyi.yu@njtech.edu.cn

S1. Experiment section

S1.1The Fabrication of Microfluidic device

The PDMS channel was fabricated using a soft lithography replica molding technique. The width of the middle channel of the PDMS channel was 300 μm and 100 μm respectively, the depth of the channel is 80 μm. The FIDTs were patterned on the substrate using a lift-off technique, the degree of arc of every FIDTs was 60°. A lithium niobate ($LiNbO_3$) wafer (double-side polished 128 Y-cut X-propagation, CAOS, CN) was selected as the piezoelectric substrate. Two thin-film metal layers (Cr/Au, 50/200 nm) were deposited on the substrate by magnetron sputtering (Explorer 14, Denton Vacuum, USA) to form the FIDTs. Finally, the photoresist was removed by acetone (99.8%, XL, CN). The FIDTs were designed to have 20 pairs of electrodes with uniform width and spacing of 25 μm, thus having a designed resonance frequency of 40 MHz. As the last step, after 40 s oxygen plasma treatment (PDC-32G, Harrick, USA), the PDMS channel and piezoelectric substrate with patterned FIDTs were aligned and heated at 150 °C for 3 h to complete the bonding.

To measure the resonant frequency of the fabricated microfluidic device, we used a vector network analyzer to do the measurement and we obtained the precise value of 35.4 MHz. It is well known that, the closer of the frequency of driving signal to the resonance frequency, the more efficient of conversion from electrical energy to FSAW energy, which induces a stronger acoustic radiation pressure. In order to obtain higher energy utilization efficiency and stronger acoustic radiation force, our experiments were conducted at this frequency.

S1.2 Device operation

In the experiment, when surface acoustic waves was needed, a sinusoidal electrical signal from a signal generator (33250A, Agilent, USA) was first amplified by a power amplifier (BA4850, NF Corporation, Japan) and then applied on the FIDTs.

S1.3 Reagents and Sample preparation

Polyvinyl alcohol (PVA, M_W =18000-26000);Sucrose; Fluorescein isothiocyanate dextran (FITC-DEXTRAN, MW = 5000); Nile Red; Sodium dodecyl sulfate (SDS);Hexadecane; 3M Novec7500,1H,1H,2H,2H-perfluorooctyltrichl-orosilane;1,2-dioleoyl-sn-glycero-3-phosphocholine (DOPC); Haematococcus Pluvialis was purchased from Nanjing Duly Biotech Co. Ltd (Nanjing, China); Polystyrene microspheres were purchased from Suzhou Nanomicro Technology Co., Ltd (Suzhou, China).

In the process of generating microcapsules with solid bead cores, the aqueous solution was prepared by mixing 10% (w/w) polyvinyl alcohol (PVA, MW =18000-26000), 2% (w/w) sucrose, PS microspheres with the diameter of 31.1μm and was injected into Inlet B. Most the PS microspheres have a nominal diameter of 31.1μm.The use of sucrose is to adjust the density of the solution to avoid the precipitation of PS microspheres to the bottom of the flow channel. The oil flow of hexadecane (HE) was prepared by mixing 5% (w/w) Span 80 and 2mg/ml 1, 2-dioleoyl-sn-glycero-3-phosphocholine (DOPC) and injected into Inlet A. In the process of generating microcapsules with droplets cores, the droplet flow was prepared by mixing the water-in-oil droplets, hexadecane, 5% (w/w) Span 80 and 2 mg/ml DOPC and injected into inlet B. The aqueous solution was prepared by mixing 10% (w/w) sodium alginate (SA) and 0.1% sodium dodecyl sulfate (SDS) and injected in inlet A as the water phase and inlet C. As a surfactant, Span 80 was added to reduce the surface tension of the fluid to more easily form multiphase laminar flow and oil/water interface. Due to the amphiphilic nature, DOPC was added to make the resulting shell structure more stable.

S1.4 Imaging acquisition

The experimental process was recorded using an image acquisition system including a microscope (M330-M100, AOSVI, China) and a high speed CCD camera (MIROEX4-4096MC, Phantom, USA). After the microfluidic generation of microcapsules, we collected

samples containing microcapsules, and then obtained their fluorescence images using a Laser Scanning Confocal Microscope (LSCM) (A1, Nikon, Japan).

S1.5 The interface tension of the oil/water interface

As a surfactant, Span 80 was added to reduce the surface tension of the fluid to more easily form multiphase laminar flow and oil/water interface. If the Span 80 was not added, the stable multiphase laminar flow and oil/water interface would not form. To form the oil/water interface, the aqueous solution containing 10% (w/w) polyvinyl alcohol (PVA, MW =18000-26000), 2% (w/w) sucrose, PS microspheres with the diameter of 31.1μm and was injected into Inlet B, and the oil flow of hexadecane (HE) containing 5% (w/w) Span 80 and 2mg/ml DOPC was injected into Inlet A. The interface tension between the aqueous solution and oil flow is 8 mNm^{-1} using a Drop Shape Analysis System (DSA100, KRUSS, Germany). If the Span 80 was not added, the multiphase laminar flow was very unstable. The Span 80 plays an important role in producing stable multiphase laminar flow. With the amphiphilic phospholipid molecules, DOPC was added to make the resulting shell structure more stable. If the DOPC was not added, the shell broke easily.

S1.6 The simulation of FSAW

The simulation result of FSAW was actuated by FIDTs using COMSOL Multiphysics 5.2a (COMSOL, Stockholm, Sweden). The simulation of surface acoustic waves on a three-dimensional geometry was done in the time domain, which was achieved by using the “Piezoelectric Devices” module. The displacement of the substrate deformation was calculated from the transient studies.

S1.7 The size distribution of the capsules

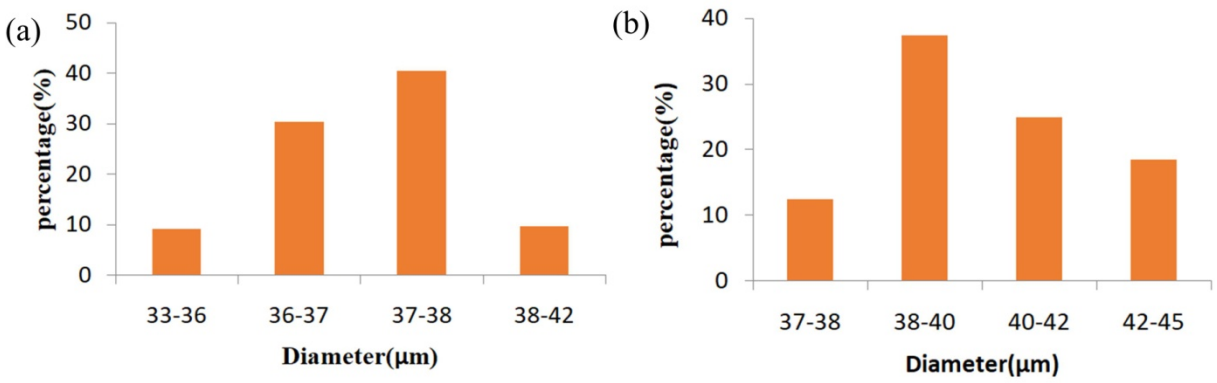

Fig.S1.(a) The size distribution of the PVA-PS microcapsules (Fig. 2Ab) with a single PVA water shell.(b) The size distribution of the HE-PVA-PS microcapsules(Fig. 2Ac) composed of a hexadecane oil shell and a PVA water shell.

When crossing the oil/water interface induced by FSAW1, the PS microspheres were encapsulated by a single PVA water shell, and the PVA-PS microcapsules were formed (Fig. 2Ab). The statistics of the size distribution of the PVA-PS microcapsules is as shown in Fig.S1(a). The size of most PVA-PS microcapsules is in the range of 36-38μm. When the FSAW2 was also on, after the PVA-PS microcapsules were generated, the PVA-PS microcapsules cross the oil/water interface again. A hexadecane oil shell was encapsulated between the PVA-PS microcapsules and the aqueous flow. The HE-PVA-PS microcapsules were generated (Fig. 2Ac). The size distribution of the HE-PVA-PS microcapsules is as shown in Fig.S1 (b).The size of most HE-PVA-PS microcapsules is in the range of 38-42μm. The size distribution of the microcapsules are summarized in Table S1.

Table S1. The statistics of the size distribution of the microcapsules

	The average diameter (μm)	**Standard Deviation (μm)**	**Coefficient of Variation (%)**
PS microspheres	31.1	0.38	1.25
The PVA-PS microcapsules (Fig. 2Ab) with a single PVA water shell	37.4	1.49	3.90
The HE-PVA-PS microcapsules (Fig.2AC) composed of a hexadecane oil shell and a PVA water shell.	41.2	2.38	5.7

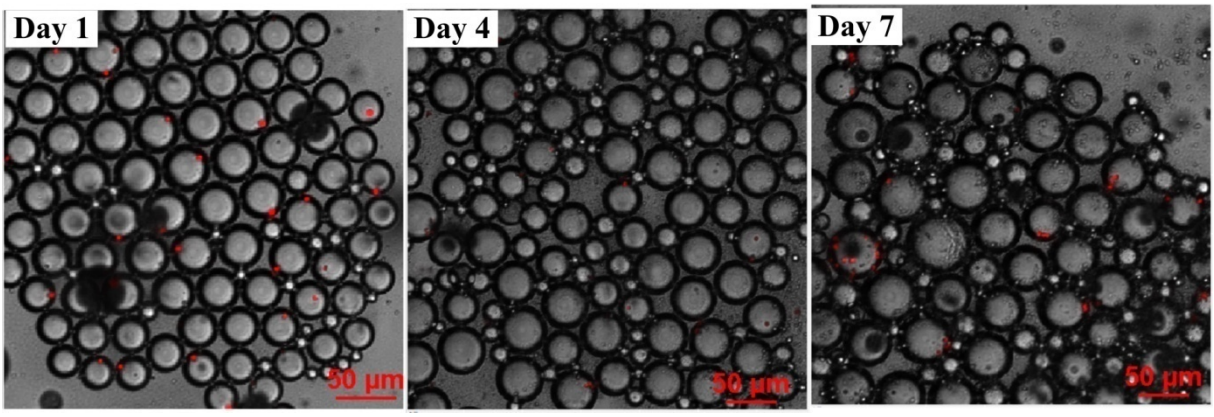

Fig. S2 The images of microcapsules with the droplets cores in different days.

As shown in Fig.S2, as the number of days increases, we found that the impurities in the sample were increasing. This was because some microcapsules were broken during the operation, but we found that most of the microcapsules were still intact after seven days.

S2. The force analysis of particle crossing the water/oil interface

In order to push the particles across the oil-water interface, the acoustic radiation force induced by FSAW has to be large enough to push the particles to overcome the main forces including stokes drag force and shear gradient lift force induced by fluid resistance and surface tension in the horizontal direction[1-3] as shown in Fig. S3. The acoustic radiation force acting on a rigid microsphere as proposed by King is defined as[4-5], $F_{SAW} = \pi R^2 \cdot \bar{E} \cdot F_F$ *for* $\bar{E} = \frac{1}{2}\rho_f k|A|^2$, $\bar{E}$ is acoustic energy density in the fluid, ρ_f is the density of the fluid, k is the wave number($k = 2\pi\lambda$) , A is the complex amplitude of velocity potential function related with the amplitude of acoustic wave, R is the radius of suspended particle in the fluid, F_F is the acoustic radiation force factor for FSAW and a rigid microsphere. Another force is shear gradient lift force,$F_L = f_L \cdot \rho_f \cdot U_m^2 \cdot R^3/H$,where $f_L$is a lift coefficient that is proportional to product of the shear rate and the shear gradient and dependent on the local shear rate, shear gradient, and Reynolds number, U_m is the maximum fluid velocity [2-3]. Stokes drag force is as $F_D = 6\pi\mu R v_x$, μ is the dynamic viscosity of water, $2R$ is the particle diameter, v_x is the lateral velocity of the particle relative to the fluid. Before the particle reaches the interface,

acoustic radiation force is merely needed to overcome the shear gradient lift force and stokes drag force. But when the polystyrene microspheres reach the oil/water interface, surface tension is added to block the crossing of the particles. According to Young-Laplace equation, the interface tension on both sides of interface can be defined by $F_\gamma = 2\pi\gamma R sin\theta$[6]. For a given frequency of FSAW, the acoustic radiation force is proportional to the square of peak-to-peak value of driving voltage (V_{pp}) ($F_a \propto V_{pp}^2$, Where F_a is the amplitude of acoustic radiation force) [7-8]. When other conditions are certain, the input frequency is 35.4 MHz, as the voltage increases, the PS microspheres with the diameter of 31.1μm showed different moving states. When the driving voltage is less than 14.5V, all the particles cannot move. When the driving voltage is between 14.5 and 21.5V, some particles can cross the interface. All the particles can cross the interface until the driving voltage is up to 21.5V as shown in Fig. S4.

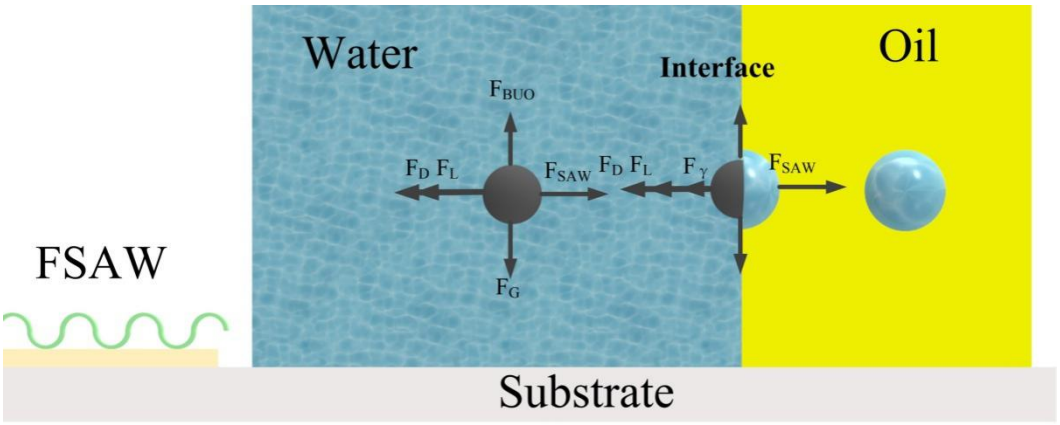

Fig. S3 The schematic diagram of the force analysis model when the particles are crossing the water/oil interface.

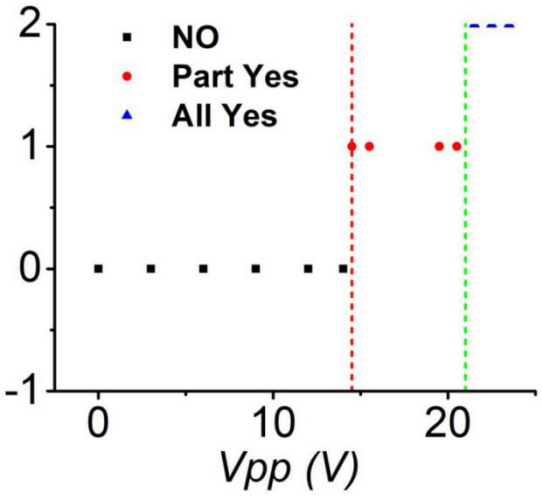

Fig. S4 The different state of particles crossing the interface as the input voltage increases. 'NO' means no particles cross the interface, 'Part Yes' means part particles cross the interface 'All Yes' means all particles cross the interface.

S3. Supplementary Movies

Video S1: When both FSAW1 and FSAW2 are on, the round-trip traveling of target particles occurs between the oil/water interfaces. The HE-PVA-PS microcapsules composed of a hexadecane oil shell and a PVA water shell were generated in this process (MP4).

References

[1] D. R. Gossett, H. Tat, K. Tse, J. S. Dudani, K. Goda, T. A. Woods, S. W. Graves, D. Di Carlo, *Small*, 2012, **8**, 2757.

[2] H. Amini, D. Di, *Lab on a Chip*, 2014, **14**, 2739.

[3] D. Di Carlo, J. F. Edd, K. J. Humphry, H. A. Stone, *Phys Rev Lett*, 2009, **102**, 094503.

[4] V. R. B. Reetu Singh, Subramanian K. R. S. Sankaranarayanan, *J Appl Phys*, 2010, **107** 024503.

[5] G. Destgeer, B. Hang, J. Park, J. Ho, A. Alazzam, *Physics Procedia*, 2015, **70**, 34.

[6] B. Moon, N. Hakimi, D. K. Hwang, S. S. H. Tsai, *Biomicrofluidics*, 2014, **8**, 052103.

[7] J. Park, J. H. Jung, K. Park, G. Destgeer, H. Ahmed, R. Ahmad, H. J. Sung, *Lab Chip*, 2018, **18**, 422.

[8]H. Bruus, Lab Chip, 2012, **12**, 1014–1021.

[9]G. Destgeer, B. H. Ha, J. H. Jung and H. J. Sung, *Lab Chip*, 2014, **14**, 4665–4672.

[10]G. Destgeer, B. H. Ha, J. Park, J. H. Jung, A. Alazzam and H. J. Sung, *Anal. Chem*, 2015, **87**, 4627−4632.

[11]G. Destgeer, A. Alazzam and H. J. Sung, *J. Mech. Sci. Technol.*, 2016, **30**, 3945–3952.

[12]G. Destgeer, H. Cho, B. H. Ha, J. H. Jung, J. Park and H. J. Sung, *Lab Chip*, 2016, **16**, 660–667.

[13]D. J. Collins and Y. Ai, *Anal. Chem*, 2016, **88**, 5513−5522.

[14]Z. Ma, D. J. Collins, J. Guo and Y. Ai, *Anal. Che*m, 2016, **88**, 11844–11851.

[15]G. Destgeer, J. H. Jung, J. Park, H. Ahmed and K. Park, *RSC Adv*, 2017, **7**, 22524–22530.

[16]Ghulam Destgeer, Jin Ho Jung, Jinsoo Park, Husnain Ahmed, *Anal. Chem*, 2017, **89**, 736−744.